

# Aerodynamic performance scaling of vertical-axis wind turbine models with Reynolds number and rotor solidity

Subrahmanyam Duvvuri\*, Mark Miller, and Marcus Hultmark

Princeton University, Department of Mechanical & Aerospace Engineering, Princeton, NJ 08544, USA

\* subrahmanyam@princeton.edu

## Abstract

The aerodynamics associated with wind turbines are of great practical significance, and present interesting fundamental problems in terms of the underlying flow physics. A primary challenge in laboratory-scale experimental studies of wind turbine models is the inability to achieve dynamic similarity with full-scale field turbines using conventional flow facilities. The present work overcomes the same by employing high-density working fluid in the form of compressed air (up to 220 bar) to experimentally investigate the performance of vertical-axis wind turbine (VAWT) models at high Reynolds numbers (up to  $5 \times 10^6$  based on the rotor diameter) that match field conditions, while simultaneously maintaining the non-dimensional rotation rates and Mach numbers in the desired range. Aerodynamic performance (turbine efficiency) data for a H-rotor VAWT model with varying rotor solidity is presented here along with a qualitative discussion on the observed behavior with Reynolds number and rotation rate.

## 1 Introduction

Wind energy is routinely harnessed at a commercial scale using horizontal-axis wind turbines (HAWTs), with rotor diameters that easily exceed 100 meters. While modern HAWT designs operate at high aerodynamic efficiencies, they are mechanically complex machines with high installation and maintenance costs. Vertical-axis wind turbines (VAWTs), also known as cross-flow turbines, provide a low-cost alternative to HAWTs and enable access to wind resources with operational advantages in a variety of environments (Dabiri, 2014; Strom et al., 2017). VAWTs present a very interesting and challenging fluid dynamical problem that combines unsteady flow and high Reynolds numbers. Unlike HAWTs, the aerodynamic performance of VAWTs is not easily amenable to simple predictive models, like the ones based on blade element momentum theory (for instance, see discussion by Lohry and Martinelli, 2016). Thereby commercially available VAWTs today rely to a large degree on empiricism and heuristics in their design, and suffer from operational inefficiencies. Modeling and design efforts of VAWTs can considerably benefit from relevant experimental studies of model turbines at realistic flow conditions.

Although VAWTs are typically designed to be smaller in size than HAWTs, they nonetheless pose significant challenges in terms of laboratory-scale experimentation. The governing flow parameters for a canonical wind turbine problem in general are the Reynolds number ( $Re_D$ ), non-dimensional rotation rate (referred to as the tip-speed ratio  $\lambda$ ), and Mach number ( $M$ ), which are defined as

$$Re_D = \frac{\rho U D}{\mu}; \quad \lambda = \frac{\omega(D/2)}{U}; \quad M = \frac{\omega(D/2) + U}{a}. \quad (1)$$

Here  $U$  is the wind speed,  $D$  is the rotor diameter,  $\omega$  is the rotor angular velocity,  $\rho$  is the air density,  $\mu$  is the air dynamic viscosity, and  $a$  is the speed of sound. Laboratory experiments with model wind turbines can capture all the flow physics and provide accurate results only when full dynamic similarity is achieved with the field operational conditions of the corresponding full-scale turbines (*i.e.* simultaneous match between the field and laboratory of all three parameters listed in equation 1). Given the high  $Re_D$  of utility-scale wind turbines and the inverse dependence on  $U$  of  $Re_D$  and  $\lambda$ , it is practically impossible to achieve full dynamic similarity with a laboratory-scale model in a conventional wind tunnel.

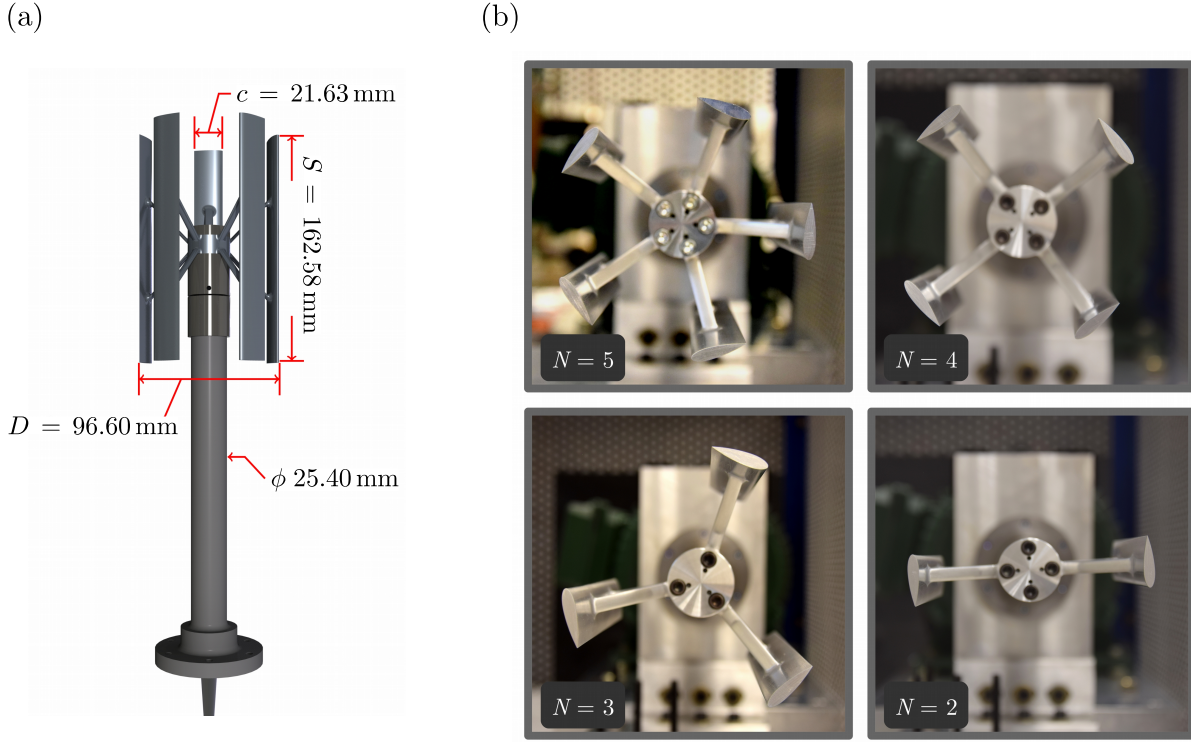


Figure 1: (a) Five-bladed VAWT model with dimensions; (b) photographs with a top-down view of the four different rotor configurations used in this study.

A novel approach to overcome this limitation was recently implemented by the authors in an experimental study of a geometrically-scaled VAWT model with a 5 bladed H-rotor configuration (Miller et al., 2018). Compressed-air was used as the working fluid in the study to obtain high Reynolds numbers by increasing  $\rho$  while maintaining  $U$  at relatively low values. This allowed for simultaneous matching of  $Re_D$ ,  $\lambda$ , and  $Ma$  with the full-scale turbine, which is 22.5 times bigger in size. In the present work we utilize the same experimental technique to understand the scaling behavior of the turbine power coefficient (non-dimensional power  $C_p$ ) with  $Re_D$ ,  $\lambda$ , and the rotor solidity ( $\sigma_N$ ), which is a key design parameter for practical turbines.  $C_p$  and  $\sigma_N$  are defined as

$$C_p = \frac{\bar{\tau} \bar{\omega}}{(1/2)\rho S D U^3}; \quad \sigma_N = \frac{N c}{D}, \quad (2)$$

where  $\tau$  is the central rotary shaft torque,  $S$  is the rotor span,  $N$  is the number of rotor blades,  $c$  is the blade airfoil chord length, and  $\bar{(\cdot)}$  denotes the time-averaging operator. The rotor solidity is varied by changing the number of blades. Details of the experiments are presented in the following section.

## 2 Experimental set up

The base turbine model used in this study is same as the one used previously. In separate sets of experiments the rotor was configured with azimuthal symmetry to have  $N = 2, 3,$  and  $4$  blades, while the rest of the turbine geometry remained unchanged. Data for  $N = 5$  with the same turbine geometry is already available from Miller et al. (2018) for comparison. This gives a range of solidities  $\sigma_N = [0.45, 1.12]$  with  $N$  going from 2 to 5. Figure 1 shows a CAD rendering of the five-bladed rotor configuration with relevant dimensions, along with photographs of the four different rotor configurations considered in this study. It is to be noted that all the turbine blades (along with the support struts) used in the present study and Miller et al. (2018) are identical, and the same tower housing was used throughout. Hence  $D$ ,  $S$ , and  $c$  remain fixed as  $N$  (and thereby  $\sigma_N$ ) is varied.

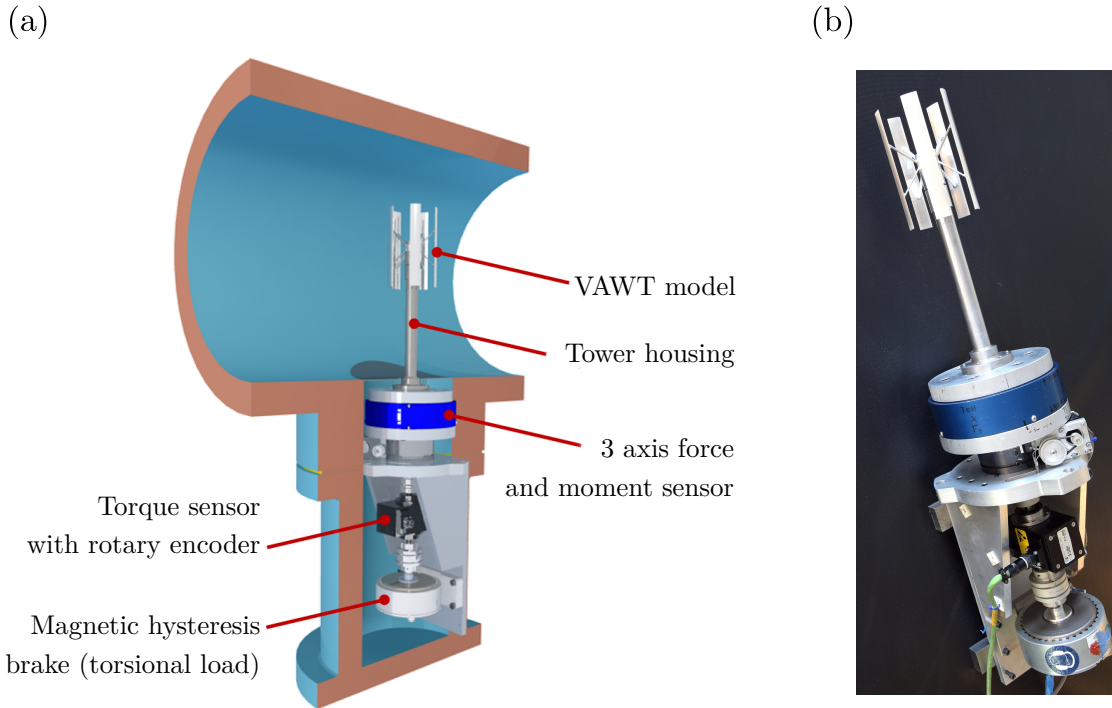


Figure 2: (a) Cut-away of the circular HRTF test section with the VAWT model and measurement stack; (b) photograph of the five-bladed VAWT model and measurement stack.

The aerodynamic performance of the models was tested at the Princeton high Reynolds number test facility (HRTF), a recirculating type compressed-air wind tunnel with static pressures ( $p_s$ ) of up to 220 bar and a maximum free-stream velocity of  $U = 10$  m/s. In that pressure range,  $\rho$  for dry air scales almost linearly with  $p_s$  whereas  $\mu$  changes only by about 30%. Hence an increase in  $Re$  by a factor of  $\approx 200$  is obtained for given length and velocity scales in comparison to a conventional wind tunnel. In addition,  $M$  remains well within the incompressible flow limit in all experiments since  $a$  is mostly insensitive to changes in  $p_s$ , and the total blade velocities remain relatively low. Further details on the facility can be found in Jimenez et al. (2010) and Miller et al. (2018). Figure 2 shows a CAD rendering of the VAWT model along with the measurement stack integrated into the HRTF test section. A central rotary shaft connects the rotor to the brake at the bottom of the measurement stack, with a force/moment transducer and a torque sensor (and a built-in encoder) connected in-line.

The rotors were solely powered by aerodynamic forces in all the experiments with no external aids for rotation. For a given  $N$ ,  $Re_D$  was set by operating the tunnel at a suitable combination of  $p_s$  and  $U$ . For a fixed  $Re_D$ , the tip-speed ratio  $\lambda$  was then varied by externally controlling the torsional brake load and thereby the rotational speed of the rotor. The mechanical power ( $\tau \times \omega$ ) extracted by the turbine was directly measured by the torque transducer and rotary encoder in a time-resolved manner. This measurement can be treated as the true aerodynamic power as mechanical losses in the setup were estimated to be minimal, and of the same order as the measurement uncertainty. The turbine configurations were tested across a large range of  $Re_D = 0.5 \times 10^6$  to  $5 \times 10^6$ . For reference, the full-scale turbine considered by Miller et al. (2018) with  $N = 5$  encounters a maximum  $Re_D$  of only  $2.4 \times 10^6$  in the field. Results from these experiments are presented in the next section, followed by a brief set of concluding remarks.

### 3 Experimental results

The power co-efficient behavior with Reynolds number and tip-speed-ratio is shown in figure 3 for the four different rotor configurations considered here. Plot markers represent experimental data points and are color-coded by Reynolds number.  $C_p$  obtained at different values of  $\lambda$  for a fixed  $Re_D$  are denoted by markers of

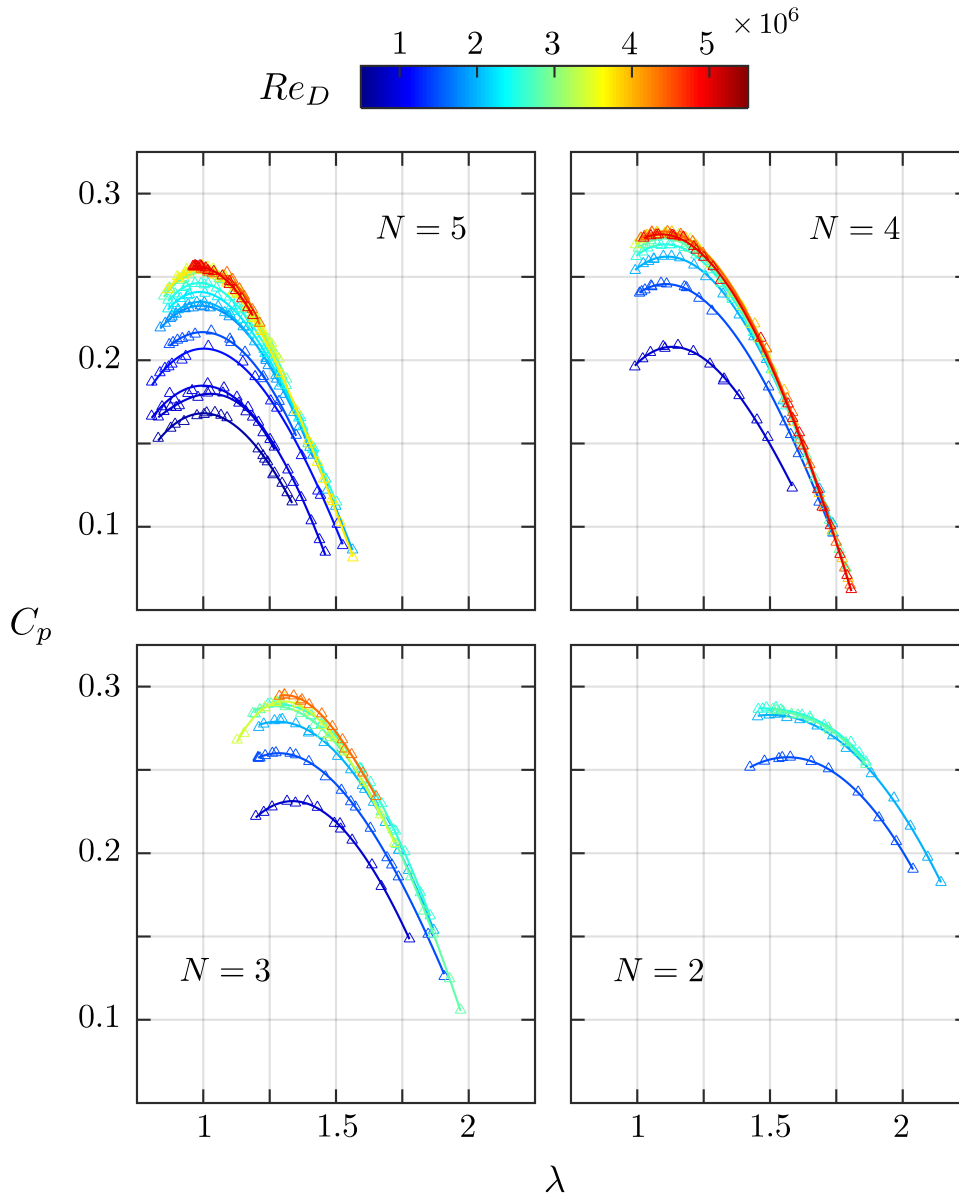


Figure 3: Power co-efficient ( $C_p$ ) behavior with Reynolds number ( $Re_D$ ) and tip-speed-ratio ( $\lambda$ ) for rotor configurations with  $N = 2, 3, 4, 5$ .

the same color. To highlight the trend of  $C_p$  with  $\lambda$  for a fixed  $Re_D$ , third-order polynomial functions are fitted to data markers and are shown as solid lines of the same color. A clear increase in turbine performance with  $Re_D$  is seen in the lower end of the Reynolds numbers range. As  $Re_D$  approaches  $5 \times 10^6$ , the curves begin to overlap one another, clearly indicating the onset of a Reynolds number invariant regime in performance. Quantitative characterization of this behavior, made possible by the present data set, has significant practical implications in terms of field turbine sizing for optimizing the overall economics of wind energy extraction.

Two clear trends are observed in the  $C_p$  data with decrease in the rotor solidity – the power curves shift upwards and towards the right while they retain the general shape. To highlight these trends, a direct comparison of  $C_p$  for  $N = 2, 3, 4, 5$  at an intermediate  $Re_D$  of  $2.82 \times 10^6$  is shown in figure 4 along with third-order polynomial fits as previously described. The maximum  $C_p$  occurs approximately at  $\lambda = 1$  for  $N = 5$ ,  $\lambda = 1.1$  for  $N = 4$ ,  $\lambda = 1.27$  for  $N = 3$ , and  $\lambda = 1.52$  for  $N = 2$ . These values of  $\lambda_{\max(C_p)}$  were found to be fairly insensitive to changes  $Re_D$  for each  $N$ , and the same can be qualitatively observed in figure 3. A simple

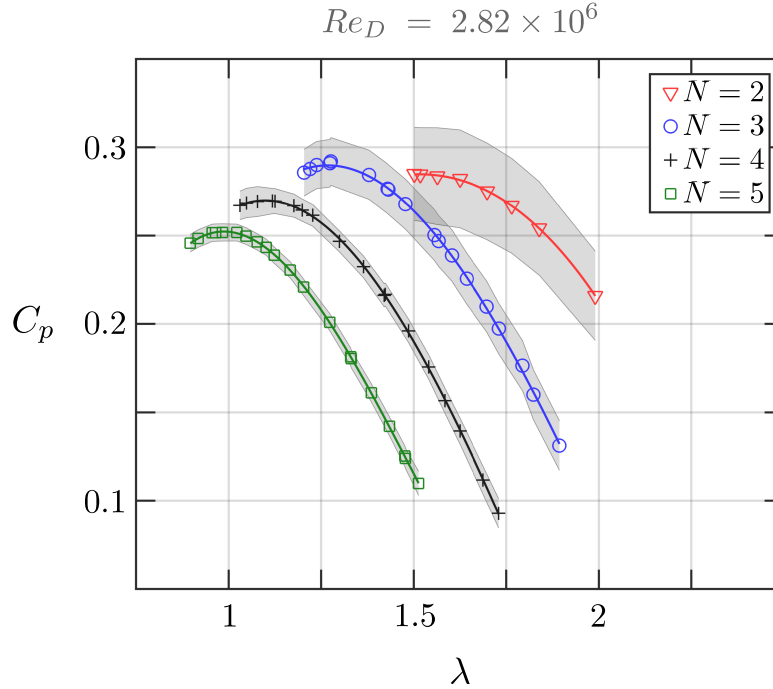


Figure 4: Power co-efficient ( $C_p$ ) behavior with tip-speed-ratio ( $\lambda$ ) for rotor configurations with  $N = 2, 3, 4, 5$  at a fixed Reynolds number of  $Re_D = 2.82 \times 10^6$ . The shaded region around each of the curves represents a conservative estimate of the total measurement uncertainty.

explanation for the rightward shift of power curves with decreasing solidity can be provided by considering changes to the effective blade Reynolds number. Decreasing solidity, or increasing porosity, results in the rotor experiencing relatively higher incoming flow momentum due to a lower blockage effect. This implies that the rotor blades operate at an effectively higher ‘free-stream’ Reynolds number, with an increase in the appropriate velocity scale. This translates to higher rotational rates and thereby higher  $\lambda$  when the far-field free-stream velocity is used to scale  $\omega$ . This also provides a partial explanation for the upward shift of the power curves with decreasing rotor solidity. The intra-cycle unsteady aerodynamic behavior of the airfoil blades needs to be considered in detail for a more complete explanation of these experimental observations, and it is the subject of future work.

On a practical note, the peak turbine efficiency goes up by about 15% when moving from a five-bladed to a two-bladed rotor as seen in figure 3. While this is attractive from a purely aerodynamic efficiency viewpoint, the higher rotational rates lead to greater structural loading. Further, lower number of blades lead to higher amplitudes of unsteadiness in intra-cycle torque loading. These considerations could possibly mitigate the advantage of higher  $C_p$  in the overall turbine operation economics. In this regard experimental data of the present kind can aid in the development of robust predictive tools for optimal design and operations of practical VAWTs.

## 4 Conclusions

The aerodynamic performance of a VAWT model with a H-rotor was systematically studied at high Reynolds numbers and varying rotor solidity. The uniqueness of the experimental technique used lies in the ability it provides to access field-scale Reynolds numbers for wind turbine aerodynamics in a laboratory setting. In the present work it allowed for the identification and characterization of a Reynolds number invariant regime in the turbine performance, and understanding the effects of rotor solidity. Experimental data of the present kind is invaluable to the modeling and design efforts of practical wind turbines. Future work with this experiment will focus on the statistical and structural nature of turbulence in the turbine wakes, and aerodynamic interactions between multiple turbines in proximity.

## Acknowledgements

Support of the National Science Foundation (grant CBET-1652583) is gratefully acknowledged. The authors also thank W. D. Kelly for assisting with the design and manufacture of the various solidity rotors used in this work.

## References

- Dabiri J (2014) Emergent aerodynamics in wind farms. *Physics Today* 67 (10): 66–67
- Jimenez JM, Hultmark M, and Smits AJ (2010) The intermediate wake of a body of revolution at high reynolds numbers. *Journal of Fluid Mechanics* 659: 516–539
- Lohry MW and Martinelli L (2016) Unsteady reynolds-averaged navierstokes simulation of crossflow rotors, scaling, and blockage effects. *AIAA Journal* 54 (12): 3828–3839
- Miller MA, Duvvuri S, Brownstein I, Lee M, Dabiri JO, and Hultmark M (2018) Vertical-axis wind turbine experiments at full dynamic similarity. *Journal of Fluid Mechanics* 844: 707–720
- Strom B, Brunton SL, and Polagye B (2017) Intracycle angular velocity control of cross-flow turbines. *Nature Energy* 2: 17103